International Journal of Mechanical and Production Engineering Research and Development (IJMPERD)
ISSN (P): 2249–6890; ISSN (E): 2249–8001
Vol. 9, Issue 6, Dec 2019, 661–672

EXPERIMENTAL CHARACTERIZATION OF POLYMER FILTER BAGS FOR PHOSPHATE DUST COLLECTOR

IKRAM LABTAINI & KHALIL EL-HAMI*

University of Sultan Moulay Slimane, Polydisciplinary Faculty of Khouribga,

Laboratory of Nanosciences and Modeling, Morocco

ABSTRACT

Filter bags used in the drying phosphate industry are made with a polymer needle felts; they are used to retrieve phosphate particles from dust air-drying before it's expelled through the smokestacks. Besides, the filter characterization has important implications for the rate of pressure losses across the filter bags. Three polymer filters used for bag house phosphate dust collectors were characterized by X-ray diffraction (XRD), X-ray fluorescence (XRF) and Raman spectroscopy. The aim of this work is to comparatively study the chemical composition of filters adopting in phosphate collectors installed in the drying unit of Beni-Idir, Khouribga, Morocco. The first sample (F1) is made with polyacrylonitrile (PAN). The second sample (F2) is the same as the first but it is in his degraded state. The third sample (F3) is an intensive filter jet with Coanda injector and combi-jet (IFJCC). The fourth sample (F4) is treated polymer filter. Results reveal that both (F1) and (F2) had an orthorhombic crystalline structure, while (F3) and (F4) had a monoclinic one. XRD suggests that (F1), (F2), and (F3) have crystallites size of 91, 72, and 66 nm, respectively. XRF and Raman spectroscopy propose that (F3) and (F4) had almost the same chemical composition. Moreover, the achieved results are generally incoherent with the expected structural characteristics reported in the literature, and the outcomes of this study could be induced to other bag house's applications.

KEYWORDS: Polymer, Filter Bag, Phosphates, Dust & Characterization

Received: Aug 29, 2019; **Accepted**: Sep 18, 2019; **Published**: Nov 15, 2019; **Paper Id**.: IJMPERDDEC201956

Original Article

1. INTRODUCTION

Polymer filter bags are extensively used in baghouse dust collectors. The larger part of advancement work that has been performed in the industry in the ten recent years, has not been in the domain of collectors development itself but in the filter fabrics industry (1). One of the most serious factors to any dust collector system is the filter's ability to capture the dust particles from the dust laden-air flows into the filter bag material in the collector. However, the filter bag is considered as the heart of the baghouse collector. While choosing the most adequate filter, a well-known of the inherent properties of the filter medium is required (2). These properties incorporate structural characteristics and elemental composition. Most recent fabrics filter bags have acquiesced to a surface treatment such as polytetrafluoroethylene(PTFE) membrane coating, calendaring etc. These treatments increase the filtration efficiency. In the treatment control, the pore size openings are smaller, so they will only allow exceedingly nanoparticles to pass, making the filter bag extremely efficient. Meanwhile, there are two stages for collecting particulates on filter media. The first is depth clogging; this is when the particles that are smaller than the pore size penetrate into the filter medium. The second is surfacing clogging, meaning the particles are deposited on the surface filter and form a "porous" cake allowing the dust to filter itself. Several authors(3)(4)(5) worked extensively on the characterization of polymer filters have given their intense use in the field of filtration. This article

investigates a comparative study of three polymer fiber filter media: one with a PTFE membrane coating, the second is an intensive filter jet with coanda injector and combi-jet (IFJCC), and the third is a treated polymer, also a degraded filter samples as the first was studied. Structural parameters and elemental composition were determined. Various techniques were used for filter characterization as X-ray diffraction (XRD), X-ray fluorescence (XRF) and Raman spectroscopy.

2. METHODS AND MATERIALS

The three filter media were examined by XRD, XRF and Raman spectroscopy. Table 1 displays the filters investigated and a series of their key parameters. These filters were prepared and produced in Intensive Filter Society located at Bouzonville (France).

Table 1: The Filter References and a Series of their Key Parameters

Filter Media	Reference	Weight (g/m²)	Filter Bag Dimensions (mm)	Air Permeability (L/dm² / min 200 Pa)	Thick-ness (mm)	Breaking Strength (daN/5 cm)	
						In length	Transversely
Sample (F1)	PAN 600 (H+V)	600	Ø 165 L5000	140	2.7	>85	>75
Sample (F2)	IFJCC 75/7-4500	550	Ø 160 L 4500	-	-	-	-
Sample (F3)	Treated Polyester	-	Ø 136 L3260	130	2.5	>65	>75

The first sample (F1) is a polyacrylonitrile filter (PAN); an acryl polymer of 600 g / m² weight with a 100% PTFE coating and is submitted to hydrophobic and oleophobic treatment. The operating temperature of the filter is 80°C and can reach a maximum value of 120°C. The second sample (F2) tested is an IFJCC type (75/7-4) medium. Its operating temperature is of 140°C, with a maximum value of 180°C. The third filter (F3) studied is a treated polyester medium with a flamed calendered felt, previously submitted to hydrophobic and oleophobic treatments. The operating temperature of the filter is of 140°C and can reach the maximum value of 180°C.

The analysis of XRD is made using a Bruker "D2 Phaser" powder diffractometer. The radiation source is Cu with both K_{alpha1} and K_{alpha2} wavelengths. Each measurement is over two theta ranges 5–90 degrees, in steps of 0.0365 degrees, measuring for 0.85 sec/step. All measurements are made at room temperature. For the measurements, a portion of each sample is cut and loaded directly into the diffractometer. The degraded filter (F2) is too thick for the diffractometer to work effectively; therefore, we took a measurement by scraping some of the loose powder off the filter and measuring that directly. Filter samples are analyzed by XRF without any pretreatment using a PANalytical Epsilon 3X spectrometer with the following features: an X-ray source of a ceramic metal tube, a rotating sample holder with 10 positions called Spinner. Raman spectroscopy analysis of dust samples is run on a DXR^{TM}2 LASER Raman microscope (Thermo Fisher Scientific) with a backscattering mode at room temperature in the range of 0–3500 cm^{-1}. The samples were excited using 785 nm laser with a resolution of 4 cm^{-1}.

A multiple-technique approach combining XRD, XRF and Raman analysis proved to be useful to better characterize the structural and chemical composition of filter bags. This information enables a better understanding of filter characteristics, but knowledge of the phase composition is also important in order to choose the appropriate coating treatment and for optimal conservation and preservation of the filters. XRD analysis was examined in order to compare between the samples regarding their lattice parameters, the profile parameters, and thickness of the crystallite. The profile-

matching tool in the fullproof program was used to obtain the crystalline information. While XRD supplies the structural details of filter materials, the fluorescence technique inspects the element filter composition. Raman spectroscopy technique is used for its capability to detect organic, inorganic, crystalline, and amorphous materials.

3. RESULTS AND DISCUSSIONS

3.1. X-Ray Diffraction

XRD spectra of the four samples were characterized by XRD and the results are shown in figure. 1, 2, 3 and 4. The XRD pattern of PAN filter(F1) as shown in figure 1 was well in agreement with the literature values(6). One intense peak of 2θ at 17 represents the orthorhombic PAN reflection with a P m mm space group. The degraded PAN filter spectra as presented in figure 2 have a strong peak at 25° (2θ). The peaks can be indexed on an orthorhombic system (P m mm space group). However, the crystal system of both filter samples (F3) and (F4) the fourth sample was confirmed to be monoclinic; space group: Pm/2. Figure 3 and 4 display XRD pattern of both samples (F3) and (F4). The patterns show large diffraction peaks. Consequently, the filter materials are amorphous. The lattice parameters and the volume are listed in table 2. Reliability factors and profile parameters are scheduled in table 3. It can be seen that the weighted profile R-factors (Rwp) has small values, meaning that the Rietveld refinement leads to a good agreement between the calculated and the experimental diagram. The thickness of the crystallite can be estimated from the full width at half maximum (fwhm) using the Scherrer formula:

$$t=0.94.\ \lambda/B.\ cos\ (\theta) \quad (1)$$

In the formula, λ is the X-ray wavelength 1.54439 Å, the B is the fwhm and θ is the Bragg angle. It was found that crystalline size was of 91.07, 72.37 and 66.13 nm for the samples (F1) (F3), and (F4) respectively, meanwhile it was of 264.69 nm for the samples (F2) (table 4), this may be due to the phenomenon of the agglomeration, since the sample (F2) is taken from the deposited layer of the used PAN filter. In this study, XRD patterns (F1), (F3), and (F4) are given in figures 1, 3, and 4. The PAN filter coated with PTFE membrane (F1) is semi crystallized polymers; it has a strong sharp peak at 17° (2θ). For the IFJCC (F3), there are three peaks in the range of 14°–28° (2θ) only the peak of 25.778° is strong, indicating that the IFJCC is amorphous polymer, as well as for the sample (F4), the polymer treated filter, the existence of three amorphous peaks confirms that the filter (F4) is amorphous. The type of filter material used in baghouses depends strongly on its structural characteristics, and the structural characteristics of filter material used in baghouses are related to the specific application and the associated chemical composition of the gas, dust loading, operating temperature, and the physical and chemical characteristics of the particulate.

Table 2: Structural Data of the Four Samples

Crystal System	Crystal System	Space Group	Lattice Parameters						Volume (V)
			a	b	c	α	β	γ	
Sample (F1)	Orthorhombic	P m mm	14.79	7.56	6.70	90	90	90	749.68
Sample (F2)	Orthorhombic	P m mm	16.60	8.50	6.44	90	90	90	909.68
Sample (F3)	Monoclinic	P 2/m	18.91	8.48	13.38	90	109.360	90	2025.54
Sample (F4)	Monoclinic	P 2/m	19.47	3.75	17.42	90	113.949	90	1163.82

Table 3: Profile Factors of the Four Samples

Samples	Profile Agreement Factor				Profile Setting		
	Rp	Rwp	Rexp	Goff	U	V	W
Sample (F1)	16.20	12	3.77	3.2	32.74	0.21	0.005
Sample (F2)	38.10	33.30	10.80	3.1	1.29	0.07	0.005
Sample (F3)	2.31	3.12	1.56	2	20.68	0.96	0.005
Sample (F4)	12.5	12.8	2.13	6	26.22	1.06	0.005

Table 4: Intense Peaks, Hkl Indices, Crystalline Size and Crystallinity of the Four Samples

Samples	Intense Peak	2θ	B	HKL	t(nm)
Sample (F1)	15148.1	17.669	0.924225	0 1 1	91.07
Sample (F2)	75.7	25.503	0.322346	4 0 1	264.69
Sample (F3)	4316.1	25.778	1.179019	3 2 0	72.37
Sample (F4)	4266.0	26.226	1.291448	0 1 2	66.13

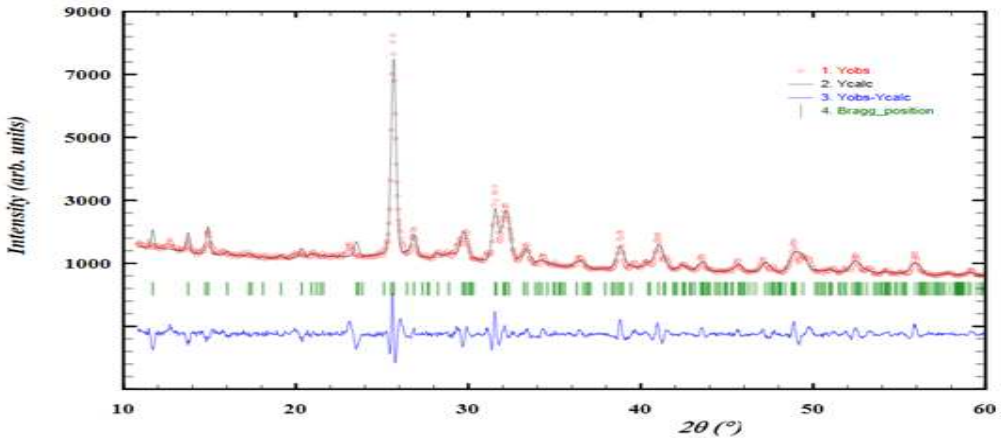

Figure 1: XRD Spectra of PAN Filter (Sample F1).

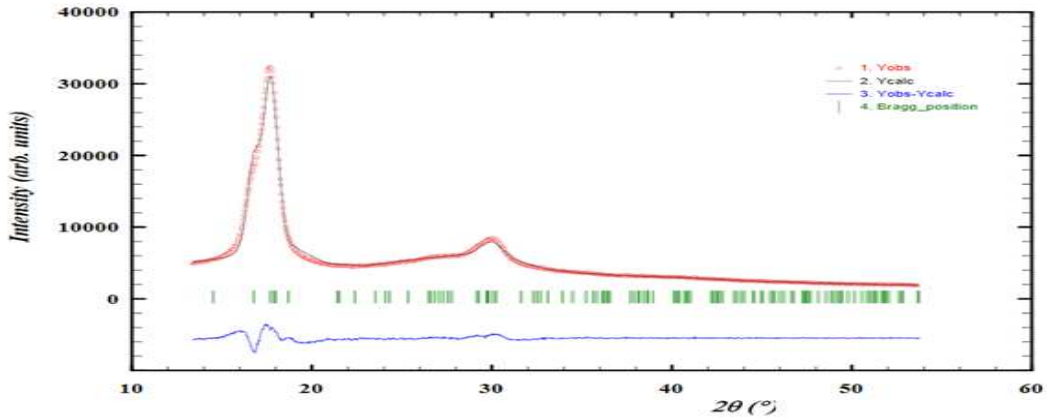

Figure 2: XRD Spectra of Degraded PAN Filter (Sample F2).

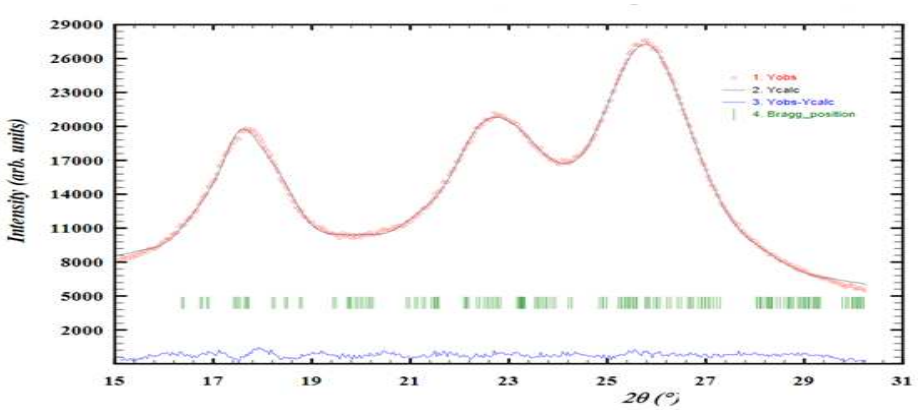

Figure 3: XRD Spectra of IFJCC (Sample F3).

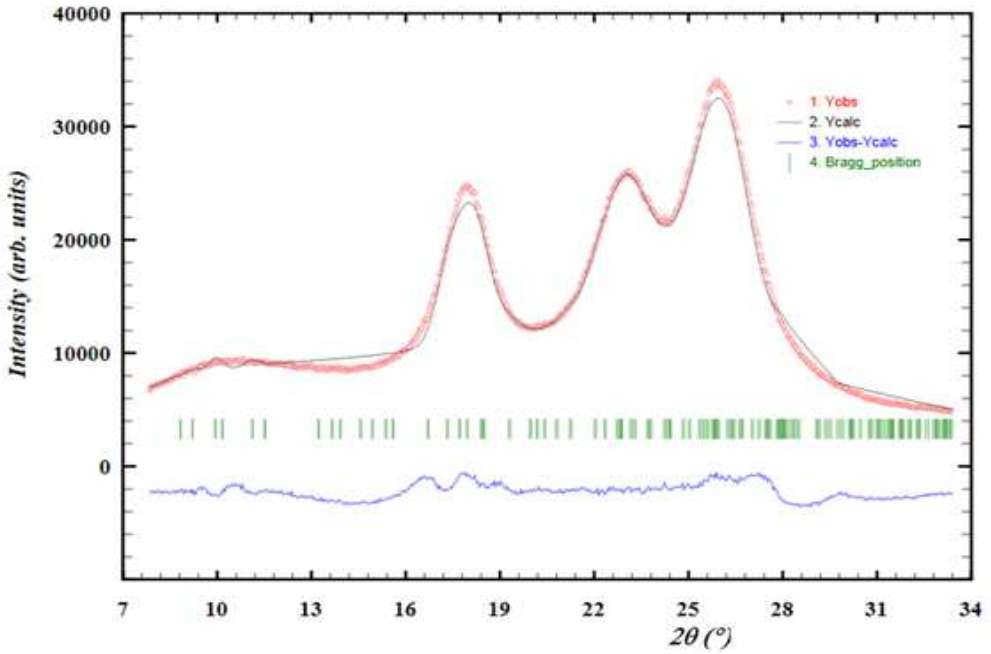

Figure 4: XRD Spectra of Treated Polymer Filter (Sample F4).

3.2. X-ray Fluorescence

We have been able to measure the chemical composition by XRF of the PAN filter media (F1), table 5 exposes the major elements obtained as well as the trace elements, according to figure 5, it can be seen that the major elements possess low energy values varying from 1 to 4 KeV, in addition all major elements belong to the Kα layer. However, the filter is made with PAN, the PAN has the chemical formula$(C_3H_3N)_x$, and these elements cannot be quantified by the XRF given their low Z atomic numbers. We also examined a sample of the same PAN filter bag used for 12 months. Figure 6shows the spectrum obtained for the sample tested, and Table 6exposesthe concentration of the detected elements, comparing these results with those which preceded, we note a significant increase in the concentration of Ca and P, thus the appearance of several trace elements, this is due to the deposition of the filter cake on the surface of the filter media. Figure 7 represents the spectrum obtained by X-ray fluorescence XF of the IFJCC (F3), an emission of observable Mα energy at a value of approximately 2.4 KeV. The major elements in the Kα layer have energy between 1 KeV and 4.5 KeV and are shown with the trace elements in table 7. Table 8 shows that the treated polymer type filter (F4) is composed mainly of Silicon, Phosphorus, Calcium, and Thallium. We can predict that it is a Si-Ti type polymer. Figure 8 concludes that all of the detected elements belong to both layers K and L. Their emission energies are between 1 KeV and 29.8 KeV.

Table 5: Element Concentration of PAN Filter (Sample F1)

Major Elements		Trace Elements	
Compound	**Concentration (%)**	**Compound**	**Concentration(ppm)**
Ca	0.626	Ag	460
Cl	0.376	Fe	375
S	0.303	Al	296
P	0.201		
Si	0.176		
K	0.148		

Table 6: Element Concentration of Degraded PAN Filter (Sample F2)

Major Elements		Trace Elements	
Compound	**Concentration (%)**	**Compound**	**Concentration(ppm)**
Ca	12.382	Mg	730
S	4.076	K	703
P	1.341	Ag	532
V	1.245	Ti	494
Si	0.678	Cr	416
Fe	0.536	Zn	379
Ni	0.199	Sr	355
Al	0.192	Cu	106
Cl	0.108	Y	96

Table 7: Element Concentration of IFJCC (Sample F3)

Major Elements		Trace Elements	
Compound	**Concentration (%)**	**Compound**	**Concentration(ppm)**
		S	994
		Al	688
Ti	1.215	Mn	666
Ca	0.595	Ag	566
Si	0.197	Fe	507
P	0.190	K	381
Cl	0.125	Mg	187
		Zn	140
		Sb	103

Table 8: Element Concentration of Treated Polymer Filter (Sample F4)

Major Elements		Trace Elements	
Compound	**Concentration (%)**	**Compound**	**Concentration (ppm)**
		Cl	699
Ti	1.300	Mn	628
Ca	0.415	Ag	570
P	0.189	Al	494
Si	0.179	Fe	375
		K	343

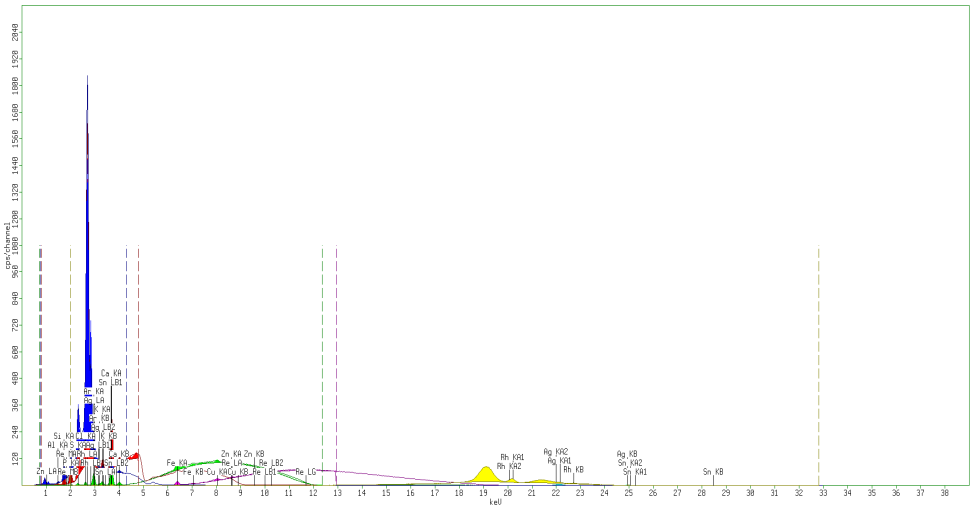

Figure 5: XRF Spectra of PAN Filter (Sample F1).

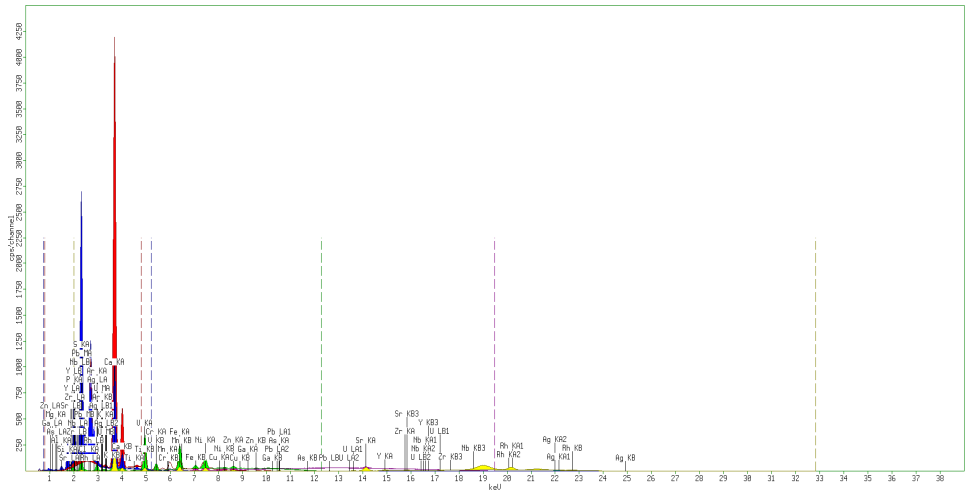

Figure 6: XRF Spectra of Degraded PAN Filter (Sample F2).

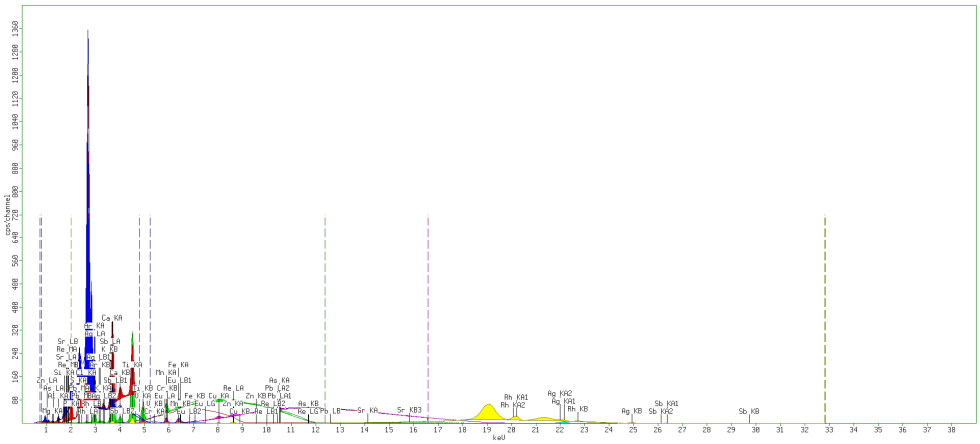

Figure 6: XRF Spectra of IFJCC (Sample F3).

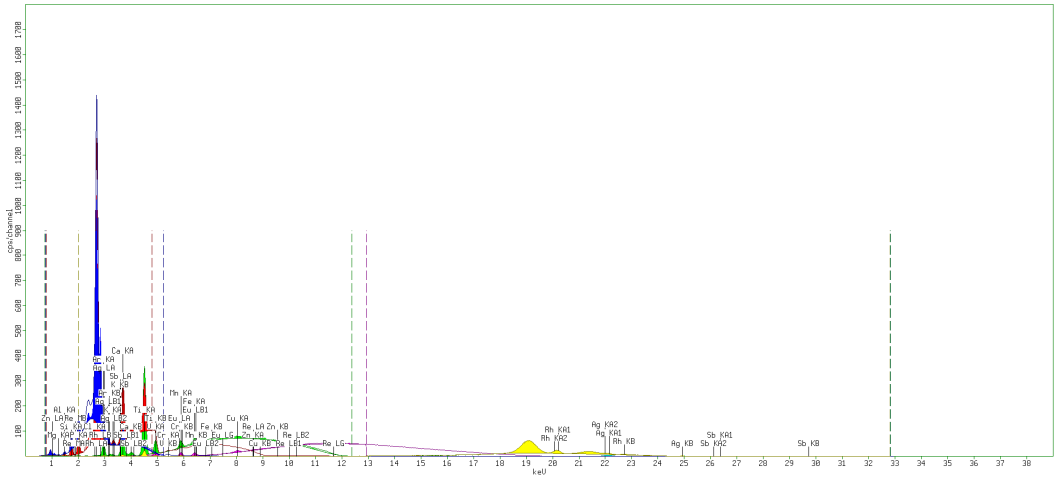

Figure 7: XRF Spectra of Treated Polymer Filter (Sample F4).

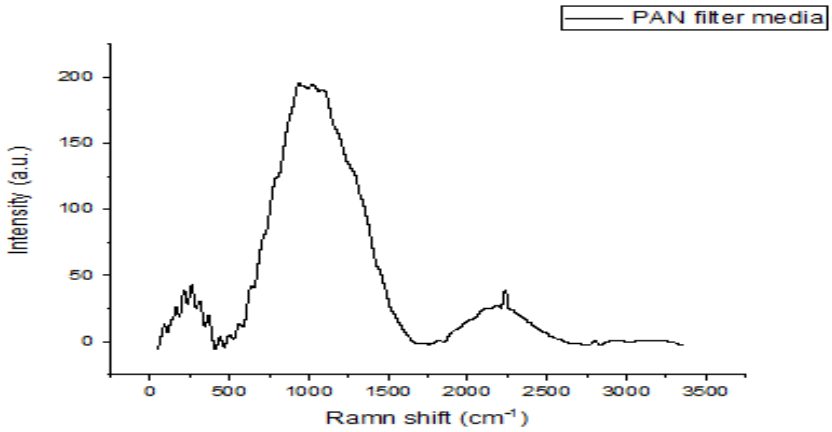

Figure 8: Raman Spectra of PAN Filter (Sample F1).

3.3. Raman Spectroscopy

Besides X-ray techniques, Raman spectroscopy was used. This technique allows the direct and non-destructive detection of chemical elements. Figure 9,10,11 and 12 show Raman spectra of the PAN filter coated with PTFE in both new and degraded state, the IFJCC and the treated polymer filter samples (F3) and (F4) in the wave number ranges 0–3500 cm^{-1}. On the one hand, the spectrum of the sample (F1) reveals three main peaks. The first band at 256 cm^{-1} might indicate the presence of C-C aliphatic chain. The second band in 1014 cm^{-1} which is the assignment of Trans-poly acetylene. And finally, the band at 2237 cm^{-1} which correspond to the nitrile band of acrylonitrile. On the other hand, the spectrum of the degraded PAN filter bag shown in figure 10 confirmed XRF results. One large intense peak was obtained at the range 946–1022 cm^{-1}. It is assigned to PO_4 vibration modes. Figure 11 and 12 show the spectra of the IFJCC and the treated polymer filters, respectively. The Raman spectra for both spectra (F3) and (F4) looks exactly the same, only the peak intensity difference is observed. The peak intensity of the samples (F4) is smaller than that of the sample (F3), this can be explained by the difference of the crystalline size, which is confirmed by the XRD results. The crystalline size of the sample (F4) is smaller than that of the sample (F3). 623 cm^{-1} peak, this is assigned to ν4 (F_2)/ClO_4^-(7). The signal of 850 cm^{-1} referred to the amorphous phase of the polymer sample (8). The peak observed in 1283 cm^{-1} corresponds to CH_2 twist regions (9). The strong peak in 1609 cm^{-1} is consigned to CC stretching modes of biphenyl which decreases with the increase in thedegree of crystallinity of polymer samples (10).

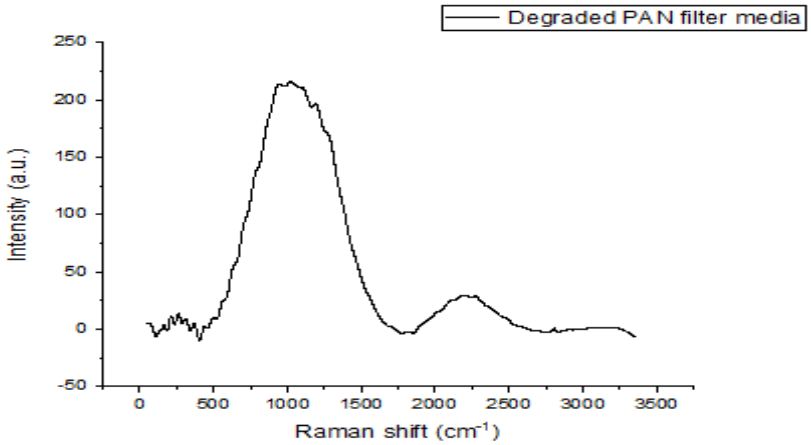

Figure 9: Raman Spectra of Degraded PAN Filter (Sample F2).

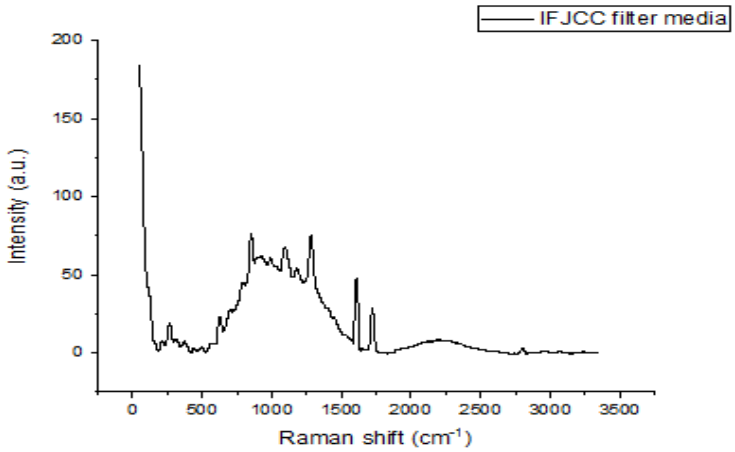

Figure 10: Raman Spectra of IFJCC (Sample F3).

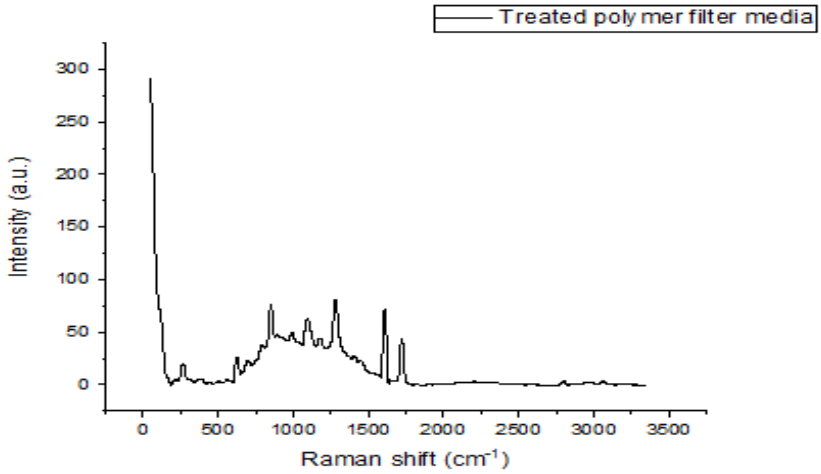

Figure 11: Raman Spectra of Treated Polymer Filter (Sample F4).

4. CONCLUSIONS

In conclusion, the present work reveals a comparative study between three types of filter bag using for phosphate dust collectors and a degraded PAN filter bag. XRD study exposes the difference in the crystallography structure. The PAN filter has an orthorhombic crystal system. The study shows that the deposit on the filtering surface has an orthorhombic crystal system and crystalline thickness of 264.69 nm due to the phenomenon of the agglomeration. The major elements in the surface deposits are Ca, S, P, and V. The share of Si, Fe, Ni, Al, Cl, and other trace elements were relatively poor. Raman spectroscopy for both samples (F3) and (F4) confirmed the XRF results. The two samples (F3) and (F4) have a similar chemical composition with little difference in the concentration elements, while XRD showed a significant change in the lattice parameters, volume and crystallite size. This study highlights the structural characteristics of polymer filters used in baghouse dust collectors, which could be extrapolated to other mining bag houses.

ACKNOWLEDGMENTS

Acknowledgments: Special thanks to Prof. Dr. J. P. Attfield and A. J. Browne from Edinburgh University, Scotland UK for the X-ray diffraction apparatus.

REFERENCES

1. *Löffler F, Dietrich H, Flatt W. Dust Collection with Bag Filters and Envelope Filters [Internet]. 1988.*
2. *Simon X, Bémer D, Chazelet S, Thomas D. Downstream particle puffs emitted during pulse-jet cleaning of a baghouse wood dust collector: Influence of operating conditions and filter surface treatment. Powder Technology 2014; 261:61–70.*
3. *Teng X, Dai J, Su J, Zhu Y, Liu H, Song Z. A High performance polytetrafluoroethene/Nafion composite membrane for vanadium redox flow battery application. Journal of Power Sources 2013; 240:131–9.*
4. *MOHAN, G. V. D., Kona, S., & NAIDU, A. L. A small-scale fabrication facility for extraction of alternative diesel fuel from waste plastic. International Journal of Mechanical and Production Engineering Research and Development, 8.*
5. *Anghelina VF, Popescu IV, Gaba A, Popescu N, Despa V, Ungureanu D. Structural Analysis of Pan Fiber by X-Ray Diffraction2010;7.*
6. *Lebedev YA, Korolev YM, Polikarpov VM, Ignat'eva LN, Antipov EM. X-ray powder diffraction study of polytetrafluoroethylene. Crystallography Reports 2010; 55(4):609–14.*
7. *Selvam AK, Nallathambi G. Polyacrylonitrile/silver nanoparticle electrospun nanocomposite matrix for bacterial filtration. Fibers and Polymers2015; 16(6):1327–35.*
8. *Di Noto V, Zago V. Inorganic-Organic Polymer Electrolytes Based on PEG400 and Al[OCH(CH[sub 3])[sub 2]][sub 3]. Journal of the Electrochemical Society 2004; 151(2):A216.*
9. *Naraghi, L., Negahban, M., & Heydari, A. The Effects of NanoParticles on Sporulation and Active Population of Talaromyces Flavus.*
10. *Carniato F, Fina A, Tabuani D, Boccaleri E. Polypropylene containing Ti- and Al-polyhedral oligomeric silsesquioxanes: crystallization process and thermal properties. Nanotechnology 2008; 19(47):475701.*
11. *Kotula AP, Snyder CR, Migler KB. Determining conformational order and crystallinity in polycaprolactone via Raman spectroscopy. Polymer 2017; 117:1–10.*
12. *Carriedo GA, García Alonso FJ, González PA, Menéndez JR. Infrared and Raman spectra of the phosphazene high polymer [NP(O2C12H8)]n. Journal of Raman Spectroscopy1998;29(4):327–30.*
13. *Santhosh, M. S., Sasikumar, R., Natrayan, L., Kumar, M. S., Elango, V., & Vanmathi, M. (2018). Investigation of mechanical and electrical properties of Kevlar/E-glass and Basalt/E-glass reinforced hybrid composites. International Journal of Mechanical and Production Engineering Research and Development, 8(3), 591–598.*

AUTHOR'S PROFILE

Prof. Dr. Khalil EL-HAMI, Born in Morocco in 1965 and earned his Ph.D in 1996 in material sciences and engineering from University of Sciences and Technology of Besancon in France. After being a Senior Research Scientist for CNRS (Centre National de la Recherche Scieitifique) of Besançon in France, he joined MaxPlank Institute of tuttgart

in Germany for synthesis and production of carbon nanotubes. From 1998 to 2005, he moved to Kyoto University in Japan as associate Professor and was promoted to full Professor Position in the Department of Electronic Science and Engineering. His major fields of study are related to nanomaterials, nanocomposites for nanosciences towards nanotechnology and components. Since 2006 at present, he has been Professor and Director of Laboratory of Nanosciences and Modeling at the University of Hassan 1st , Faculty of Khouribga in Morocco. Prof. Dr. Khalil El-Hami is member of several boards and committees, including Editor and associate Editor of international scientific journals. He earned the first price of idea contest of Kyoto University in 1999 in Japan. He has 2 patents protected in TLO and JPO, Technology Licensing Organization, and Japanese Patent Organization, and over 120 refereed international publications (including nature publishing group in September 2017) and communications with over 1400 citations.

Ikram LABTAINI, born in Morocco in 1993 and earned his state engineer diploma in 2016 in process energy and the environment from ENSA in Agadir, Morocco. Since November 2016 she has started her Ph.D. studies at the laboratory of Nanosciences and Modeling at Polydisciplinary Faculty of Khouribga in Morocco. Her major fields of study are related to nanomaterials, process engineering, and modeling. She earned the Best Award of " Young Researchers Days " Competition in « Phosphate Days 2018 » for the thesis project « Study of the pulse-jet cleaning of baghouse dust collector in O.C.P to improve the filtration performance and pneumatic cleaning optimization» at Mohammed VI Polytechnic University, Benguerir, Morocco. She earned also the “Best Paper Award” for the paper entitled « Individual element mapping of baghouse phosphate dust collector deposits » Technologies and Materials for Renewable Energy, Environment and Sustainability (TMREES19-Gr Int’l Conference), Athens, Greece. She has two published articles in indexed journals, three proceeding papers, and six oral communications in national and international conferences.